Supplementary Information

Ultra-stable $CsPbBr_3$-embedded polymer films for spectrally tunable X-ray nuclear batteries and flexible radiation imaging applications

Dongdong Liang, [a] Zhiheng Xu, [*ab] Dandan Yang [*c], Zhibin Xu, [a] Weitong Yin, [a] and Xiaobin Tang [*ab]

[a] *Department of Nuclear Science and Technology, Nanjing University of Aeronautics and Astronautics, Nanjing 211106, China*

[b] *Key Laboratory of Nuclear Technology Application and Radiation Protection in Aerospace, Ministry of Industry and Information Technology, Nanjing 211106, China*

[c] *Institute of Innovation Materials and Energy, School of Chemistry and Chemical Engineering, Yangzhou University, Yangzhou, 225002, China*

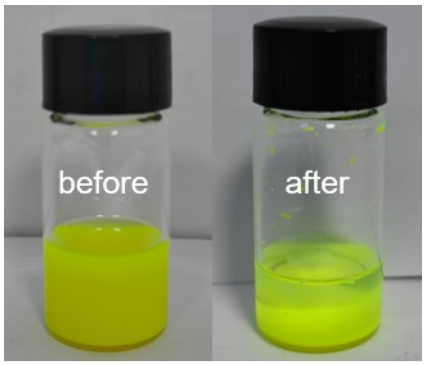

Fig. S1 Layering aggregation phenomenon of $CsPbBr_3$ nanowires (NWs).

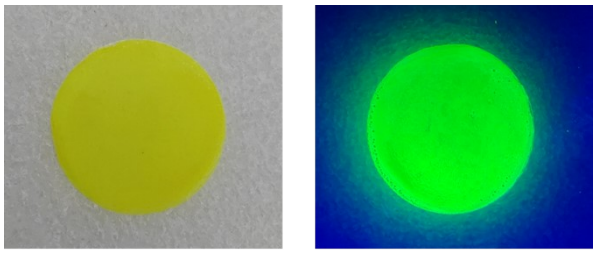

Fig. S2 Unevenness of the $CsPbBr_3$ film prepared by drop the solution of $CsPbBr_3$ nanowires onto a clean glass substrate and dry it naturally.

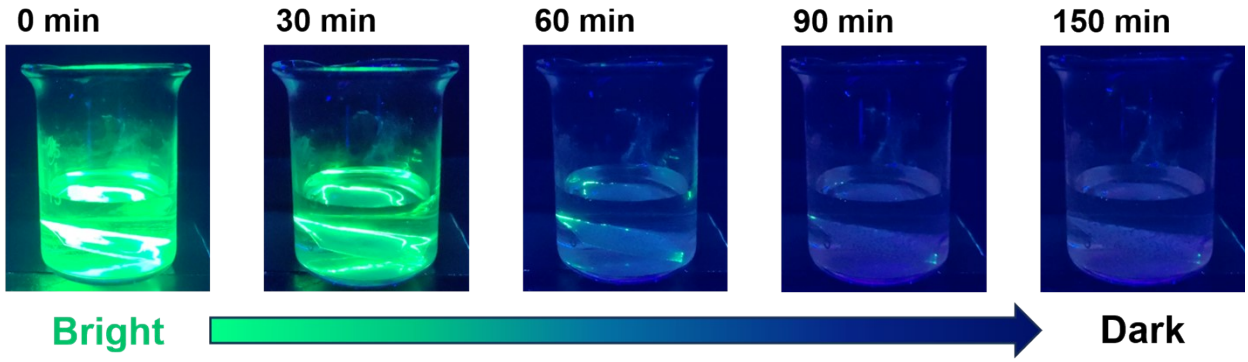

Fig. S3 Photographs of $CsPbBr_3$ nanowire films in water under 365 nm excitation.

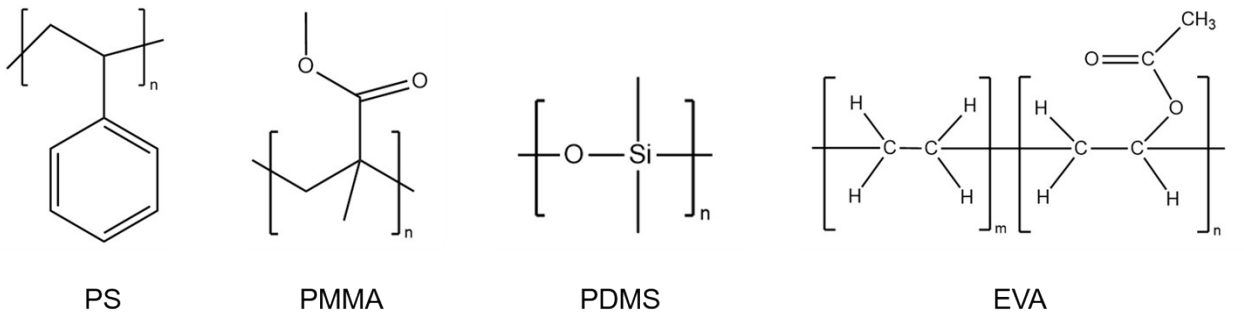

Fig. S4 The molecular formulas of polystyrene (PS), polymethyl methacrylate (PMMA), Polydimethylsiloxane (PDMS), and ethylene-vinyl acetate copolymer (EVA).

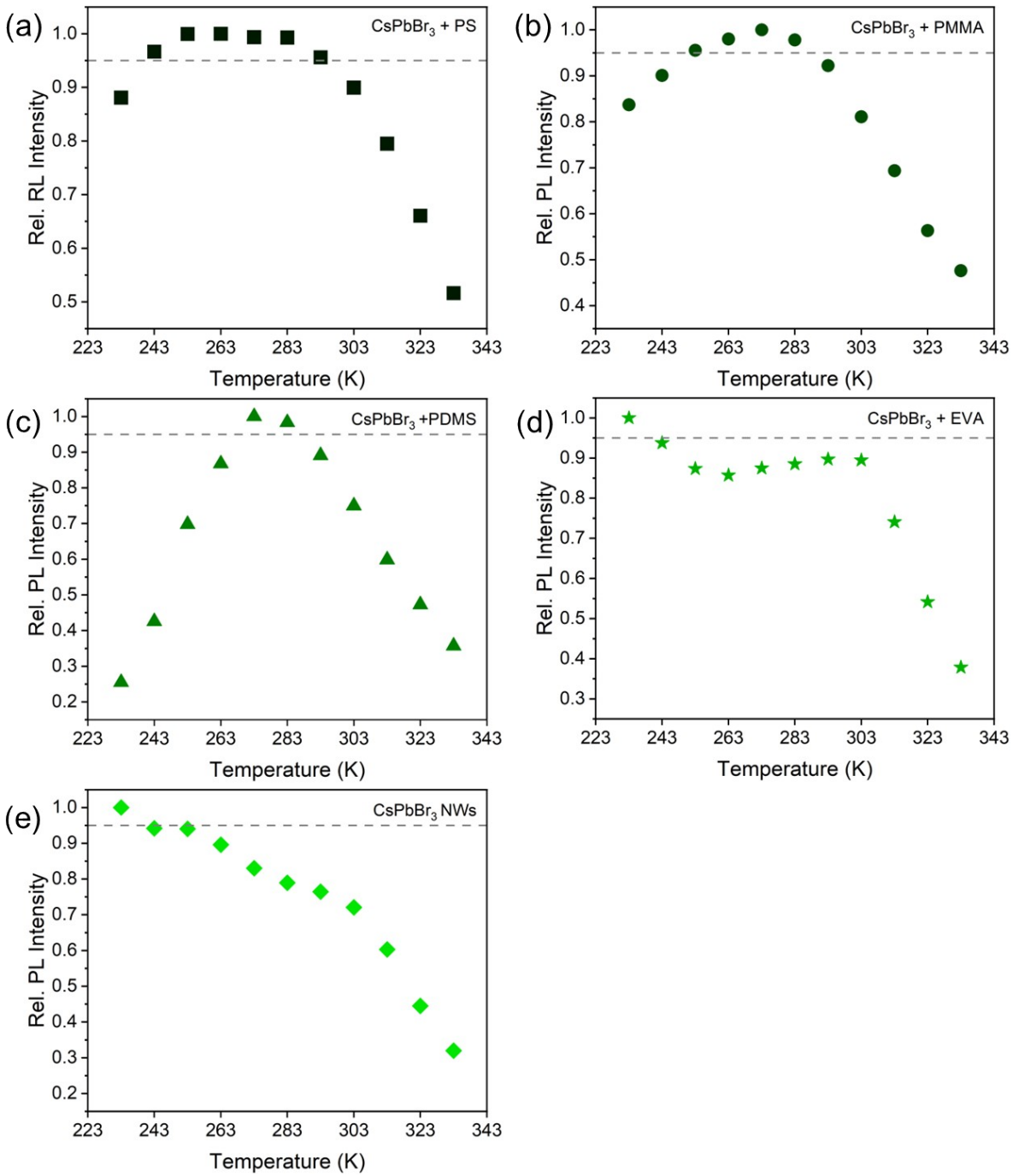

Fig. S5 Variation in photoluminescence (PL) intensity of $CsPbBr_3$-embedded polymer films and $CsPbBr_3$ NWs as a function of temperature under 365 nm excitation.

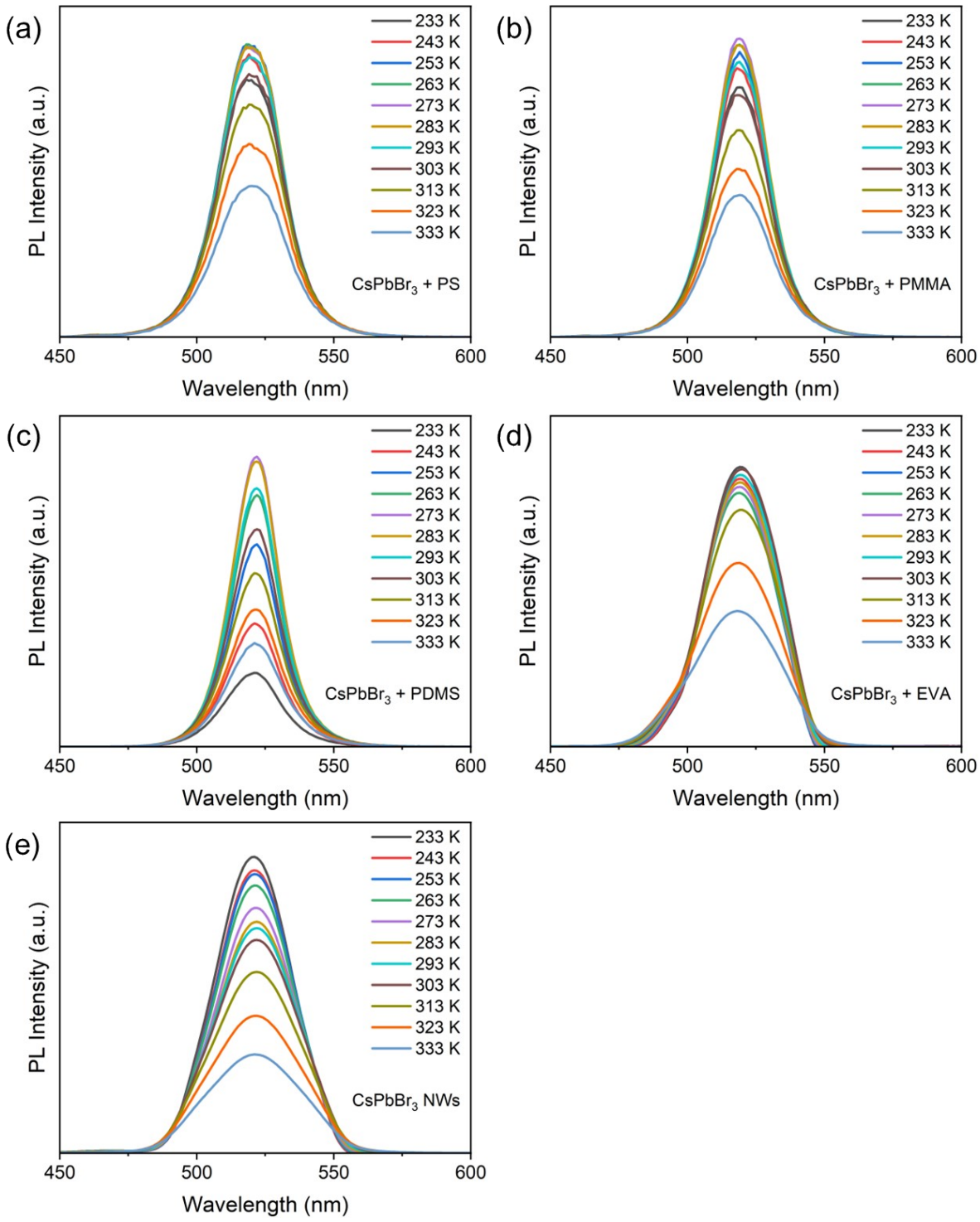

Fig. S6 Temperature-dependent PL spectra of $CsPbBr_3$-embedded (a) PS, (b) PMMA, (c) PDMS and (d) EVA film, and (e) $CsPbBr_3$ NWs.

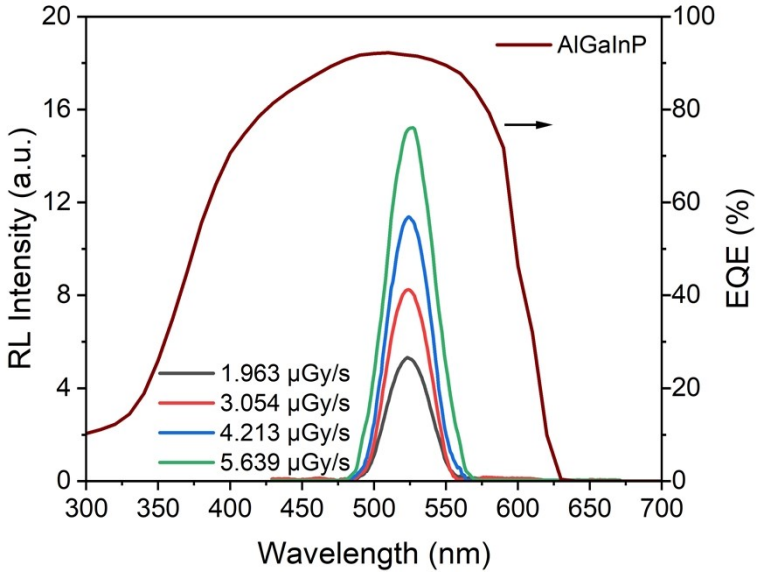

Fig. S7 Radioluminescence (RL) spectra of $CsPbBr_3$-embedded PS films under different exposure of X-ray radiation and external quantum efficiency (EQE) curve of AlGaInP photovoltaic module.

Calculation method for energy conversion efficiency of nuclear batteries

The energy conversion efficiency (η) of the nuclear battery can be expressed as:

$$\eta = \frac{P_{\max}}{P_{\mathrm{X-ray}}} = \frac{V_{\mathrm{mp}} \times I_{\mathrm{mp}}}{P_{\mathrm{X-ray}}} \qquad \text{* MERGEFORMAT (S1)}$$

where $P_{\max}$ is the maximum output power of the battery, which is the maximum value of the product of the current and voltage in the *I-V* characteristic curves, V_{mp} and I_{mp} are the corresponding current and voltage at the maximum power value, $P_{\text{X-ray}}$ is the power emitted by the X-ray tube, and this value is calculated as 1.305 mW in this work[1]. Specifically, the X-ray intensity ($I_{\text{X-ray}}$) generated at the tungsten target of the X-ray tube can be expressed as:

$$I_{\mathrm{X-ray}} = 0.9 \times V^2 \times I \times Z \qquad \text{* MERGEFORMAT (S2)}$$

where V is the X-ray tube voltage (kV), the value in this work is 30, I is the X-ray tube current (mA), the value in this work is 1, and Z is the atomic number of the X-ray tube target (tungsten, Z=74). Therefore, the power generated by the tungsten target of the X-ray tube can be calculated as 0.06 W. The X-ray energy spectrum in this state is shown in Figure S8, and it can be seen that the average energy of X-ray particles is 99.27 keV. Assuming that the X-ray particle energy emitted by the tungsten target is the average energy, the number of X-ray particles emitted by the tungsten target per second is approximately 3.77×10^{12}. The MCNP5 program was used to simulate and calculate the number of the emitted X-ray particles, and the parameters set by the model are consistent with the experiment. The distance between the beryllium window and the tungsten target is set to 3.1 mm, the thickness of the window is 200 μm, the diameter of the target is 1 mm, and the radiation angle is 20°. The calculated number of particles emitted from the X-ray tube is approximately 8.21×10^{10}, with a power of 1.305 mW.

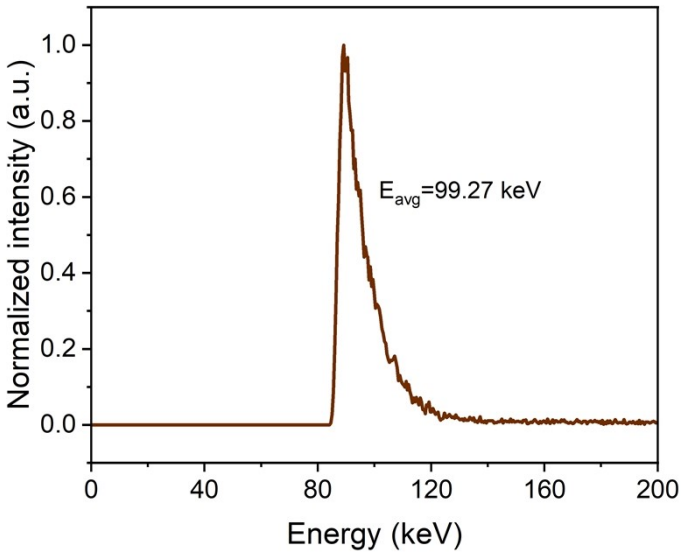

Fig. S8 X-ray energy spectrum emitted from X-ray tube.

Supplementary references

1 Z. Xu, Z. Jin, X. Tang, Y. Liu, X. Guo, C. Peng and H. Wang, *Int. J. Energy Res.*, **44**, 508–517.